The International Journal of Advanced Manufacturing Technology (2019) 103:91–100
https://doi.org/10.1007/s00170-019-03474-y

ORIGINAL ARTICLE

Modeling machining errors for thin-walled parts according to chip thickness

Caixu Yue[1] · Zhitao Chen[1] · Steven Y. Liang[2] · Haining Gao[1] · Xianli Liu[1]

Received: 3 September 2018 / Accepted: 18 February 2019 / Published online: 15 March 2019

Abstract
In the milling process of titanium alloy thin-walled parts, because of its low stiffness, processing deformation easily occurs, which results in in low-dimensional accuracy of machined surface and affecting the workpiece performance. Cutting force is the main factor that causes cutting deformation. Cutting deformation also affects cutting force. There is a coupling relationship between them. To solve the above problems, a method is proposed to predict the surface error by calculating the milling force by varying the chip thickness and by coupling the force with the elastic deformation of the workpiece. Firstly, the analytical model of bending elasticity deformation of thin-walled parts is established. Then, the micro-unit entrance angle and instantaneous chip thickness are calculated by the contact relationship of workpiece deformation and the chip boundary decision conditions. The cutting force and workpiece deformation at random rotating angle are obtained by iterative calculation method. Finally, the surface error is predicted by calculating the deformation matrix and the principle of surface generation mechanism. The simulation results are in good agreement with the experimental results, which verifies the accuracy of the proposed method. The results provide theoretical support for milling process optimization and profile accuracy control of titanium alloy thin-walled parts.

Keywords Titanium alloy milling · Thin-walled parts · Milling force · Elastic deformation · Chip thickness · Error prediction

1 Introduction

There is an increasing demand for thin-walled parts in aviation field because that they can meet the requirements of high specific strength, high specific stiffness, and high fatigue resistance of aeronautical parts. Due to the low stiffness and large size of thin-walled parts and the large amount of metal removal, poor surface quality is caused by milling force and workpiece deformation in manufacturing. The unsatisfactory processing accuracy limits the production efficiency and reduces the assembly accuracy, which has become a difficult problem in the development of aeronautical manufacturing.

Surface errors are mainly caused by deformation generated by the milling force during the machining process. The performance of workpiece materials, tool wear, and chatter of machining system will have an important impact on the formation of surface errors. Therefore, the key to predict the surface errors of thin-walled parts is to model and analyze the dynamics and deformation of the instantaneous contact relationship between workpiece and tool. Surface errors can be calculated by using finite element methods (FEM) and analytic modeling. WAN [1, 2] establishes the prediction method of machining errors in thin-walled parts milling process by finite element method to compare the rigid and flexible models. Three-dimensional irregular volume elements are obtained, which can be used to predict the shape errors of workpieces. Ratchev [3] predicts workpiece deformation by cutting force and tool deflection finite element model of adaptive theory based on workpiece deformation recognition method and key processing characteristics of tool force deflection model, which provides input value for error compensation of later prediction. Chen [4] proposes a unified analytical cutting force model based on a predictive machining theory for variable helix end mill considering cutter runout. In order to

✉ Caixu Yue
yuecaixu@hrbust.edu.cn

[1] The Key Laboratory of National and Local United Engineering for "High-Efficiency Cutting & Tools", Harbin University of Science and Technology, Harbin 150080, China

[2] George W. Woodruff School of Mechanical Engineering, Georgia Institute of Technology, Atlanta, GA, USA

reduce the machining deformation, Gao [5] has established a cutting force model and obtained a reasonable combination of cutting parameters that directly affect the machining deformation. An effective compensation theory based on modified tool location has been proposed to plan the deformation control method of tool path. Li [6] predicts the time-varying stiffness of thin-walled parts by means of structural stiffness modification method and avoids repeated cutting by means of the initial finite element model of workpiece. Lin [7] proposes a novel cutting forces and tool deflection prediction methodology for general flexible micro end mill in micromilling, which includes the effect of exact trochoidal trace, tool run-out, and deflection feedback together. Budak [8, 9] adopted the variable stiffness finite element model of workpiece. Considering the contact relationship between tool and workpiece caused by static displacement, the model of milling force and surface location error was established, and the dynamic model of workpiece in milling process was established. In the finite element calculation of cutting deformation, the accuracy of the model and the factors such as boundary and load conditions have a great influence on the calculation accuracy.

In the research of predicting surface error by analytical modeling, Yang [10] proposed a new method to analyze milling force based on the shape feature of single-edge end milling tools and classified it into three categories. Then, multi-edge end milling tools were classified by considering the cutting type of single-edge end milling tools and the tool-workpiece contact angles in cutting. Desai [11] correlates the axial and radial contact relationship between the tool and the workpiece with the cutting conditions, and presents a method for calculating the surface error distribution. Denkena [12] reconstructs the milling surface morphology by measuring the milling force. Zheng [13] establishes an analytical model of surface error considering the flexible characteristics of workpiece, tool, and machine tool. It is concluded that the cutting force pushes the tool away from the workpiece to form a positive error at a smaller cutting depth. While the cutting force pulls the tool toward the workpiece to produce an oversize cutting phenomenon at a larger cutting depth, which results in a negative error. Based on the relationship between milling forces/moments and instantaneous undeformed chip thickness, Zhang [14] has built an analytical model for end milling surface geometric error with considering cutting forces/moments to predict the surface geometric error in the end milling conditions. Kline [15] predicts surface errors according to cutting conditions and tool-workpiece geometry/material properties by combining the cutting force model of end milling with tool deflection and workpiece deformation model. Song [16] builds a three-dimensional cutting force model of the whole tool based on discrete tool model and vector superposition, and constructs a prediction model of the tool yield error and the cutting force flexibility of rigid workpiece surface with the feedback of the law of the influence of tool deformation on the milling process. Eksioglu [17] proposed that the discrete-time model can replace the flutter stability of cutting tools with various geometric shapes and can predict complex numerical simulations such as cutting forces, vibration, chip thickness, and surface position errors. Yue [18] has concluded the method for avoiding chatter in cutting process, which leads to better surface precision, higher productivity, and longer tool life.

In the process of building the cutting force model, all the above analytical methods assume that the instantaneous undeformed chip thickness is a fixed value, and the coupling relationship among cutting force, workpiece deformation, and chip thickness is not considered comprehensively, which is inconsistent with the actual processing and affects the prediction accuracy of machining errors. Dépincé [19] has calculated milling force coefficients by approximate polynomial and least squares method to establish a tool deformation error model. Considering the tool-workpiece contact point and the movement rule of cutting edge, a surface error model is built. Wan [20] has built instantaneous undeformed chip thickness model to calculate cutting force based on the relative position between the centers of two adjacent tool teeth, which could quickly identify the contact relationship between cutting edge and workpiece.

In order to further improve the accuracy of surface error prediction in thin-walled parts milling, this paper builds a milling force prediction model with variable chip thickness based on the elastic deformation principle of thin-walled parts. The workpiece deformation is calculated by iteration method, and the surface error of thin-walled parts is predicted by using the principle of surface generation mechanism and the workpiece deformation matrix. The validity of the surface error prediction model is verified by comparing with the experimental results.

2 Modeling milling force and the elastic deformation of thin-walled parts

2.1 Modeling milling force

In thin-walled parts milling, milling force is the main factor of workpiece deformation. In this paper, a milling force model is built by geometric analysis method. The model considers that the whole cutting physical process occurs in the shear zone, and the force produced by the shear slip of the workpiece material in the shear zone is the overall cutting force, so the cutting force is expressed as a proportional function of the chip load, and the proportional coefficient is named as the cutting force coefficient. In the milling process, the cutting edge is discretized into a finite number of axial disc elements with equivalent length $z_{i,j}$, and the cutting resultant force is obtained by integration. Therefore, according to the instantaneous rigid force model [21] proposed by Altintas, the

relevant tangential, radial, and axial cutting forces of the *j*th disc element of the first cutting edge are obtained as follows:

$$\begin{aligned} F_{T,i,j}(\varphi) &= K_{T,i,j}(\varphi)h_{i,j}(\varphi)z_{i,j} \\ F_{R,i,j}(\varphi) &= K_{R,i,j}(\varphi)h_{i,j}(\varphi)z_{i,j} \\ F_{A,i,j}(\varphi) &= K_{A,i,j}(\varphi)h_{i,j}(\varphi)z_{i,j} \end{aligned} \tag{1}$$

where $F_{P,i,j}$ (φ) is the tangential, radial, and axial unit milling force acting on the tooth segment (i, j) when φ, $P = T, R, A$ (T stands for tangential, R for radial, and A for axial); φ is the tool rotation angle; $h_{i,j}$ (φ) is the nominal chip thickness corresponding to the segment (i, j) of φ, which is equal to the height of the matching unit beam segment; $Z_{i,j}$ is the nominal chip width corresponding to the tooth segment (i, j) of φ; and $K_{P,i,j}$ (φ) is the instantaneous milling force coefficient, $P = T, R, A$.

The unit forces $F_{P,i,j}$ acting on each tooth layer can be transformed into $F_{Q,i,j}(Q = X, Y, Z)$ using Cartesian coordinates, and then expressed as

$$\begin{aligned} &\left[F_{X,i,j}(\varphi), F_{Y,i,j}(\varphi), F_{Z,i,j}(\varphi)\right]^T \\ &\quad = T\left(\theta_{i,j}(\varphi)\right)\left[F_{T,i,j}(\varphi), F_{R,i,j}(\varphi), F_{A,i,j}(\varphi)\right]^T \\ &\quad T(\varphi) = \begin{bmatrix} \sin(\varphi) & -\cos(\varphi) & 0 \\ \cos(\varphi) & \sin(\varphi) & 0 \\ 0 & 0 & 1 \end{bmatrix} \end{aligned} \tag{2}$$

The tool rotation angle φ can now be selected and the combined forces in the X, Y, and Z direction can be expressed as

$$F_X(\phi) = \sum_{i,j} F_{X,i,j}(\phi)\ F_Y(\phi) = \sum_{i,j} F_{Y,i,j}(\phi)\ F_Z(\phi) = \sum_{i,j} F_{Z,i,j}(\phi) \tag{3}$$

2.2 Modeling of workpiece deformation

According to the deformation characteristics of low stiffness workpiece, the elastic deformation model of thin-walled parts in milling process system is built. Based on the theory of bending and torsion elasticity, the analytical formula of workpiece elastic milling deformation is deduced [22]. The elastic milling deformation of low stiffness workpiece will occur when it is subjected to milling force. There is mainly the bending and twisting elastic deformation caused by milling force. The thin-walled parts are divided into two independent geometric parts: the unprocessed and the processed. The elastic deformation of the thin-walled parts is calculated. The expression of the elastic deformation of the thin-walled parts is as follows:

$$\delta_{\mathrm{m}} = \delta'_{\mathrm{H-ap}} + \delta_{\mathrm{ap_0}} \tag{4}$$

where $\delta'_{H\text{-ap}}$ is the unprocessed deflection variable; and δ_{ap0} is the processed deflection variable.

The bending elastic deformation of the workpiece is caused by cutting force $F_{S,i,j}$ (φ) at the height of ap_0 from the workpiece holding datum. The expression of bending deformation of thin-walled parts is deduced as follows.

$$\delta'_{H-\mathrm{ap}} = \frac{F_{S,i,j}(\varphi)(H-\mathrm{ap})^3}{3EI_1} + \frac{F_{S,i,j}(\varphi)(H-\mathrm{ap})^3}{2EI_1} + \frac{\varphi R F_{S,i,j}(\varphi)(H-\mathrm{ap})^2}{\tan\beta^* 2EI_1} + \frac{F_{S,i,j}(\varphi)(H-\mathrm{ap})^2}{EI_1} \quad (S = x, y) \tag{5}$$

$$\delta_{\mathrm{ap0}} = \frac{F_{S,i,j}(\varphi)(\mathrm{ap}_0)^3}{EI_2} \tag{6}$$

where E is the elastic modulus of the workpiece material; I_1 is the moment of inertia at which material has not been removed from the workpiece; I_2 is the moment of inertia at which material has been removed; and H is the height of the workpiece.

3 Prediction of machining errors for the side milling of thin-walled parts

The milling force of thin-walled parts is closely related to the dynamic elastic deformation of the milling process system and it has a nonlinear relationship. In the dynamic milling force model, the milling force makes the workpiece with low stiffness deviate from the ideal cutting position and changes undeformed chip thickness, which is fed back to the cutting system and the new instantaneous milling contact relationship. The dynamic deformation mainly affects the entry angle and instantaneous micro-element thickness in milling. In this paper, the change of instantaneous thickness and entry angle of side milling micro-element is studied, and the force-deformation coupling relationship of side milling process system for low rigidity parts is established.

3.1 Predicting the cutting entry/exit angle

In the process of Side Milling Thin-walled parts, each tool tooth is in the process of continuous cutting. Therefore, it should be calculated from the cutting point in the calculation of instantaneous cutting thickness. The micro-elements involved in cutting cause deformation δ_m of the workpiece, thus affecting the entry angle φ_{en} of the next micro-elements involved in cutting, as shown in Fig. 1. The micro-element cut-out angle φ_{ex} is calculated iteratively based on the

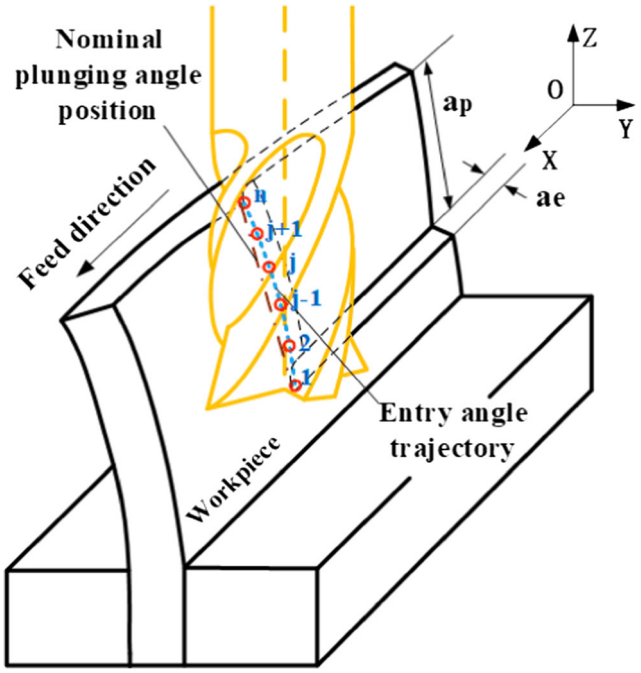

Fig. 1 Workpiece deformation affects the entry angle of the disc element

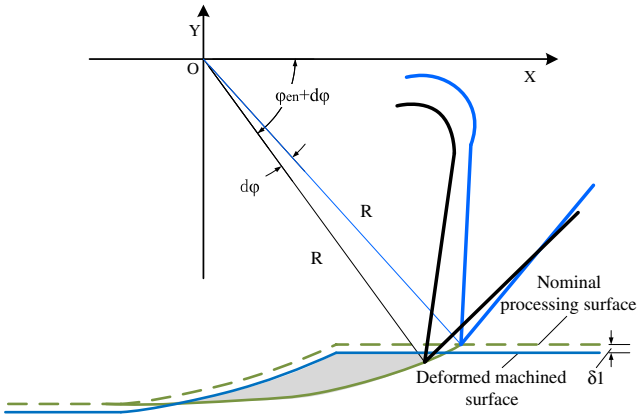

Fig. 2 Workpiece deformation changes the disc element entry angle

instantaneous chip thickness, workpiece deformation, and chip boundary conditions.

In the process of thin plate flank milling, the path of the entry point of the workpiece is straight line, and the position of the entry point is the same as that of the feed per tooth. Because the thin-walled parts are deformed by milling force in the radial direction of the cutter, the entry angle of the i+1th cutter tooth increases, so that the entry distance of each micro-element cutting edge is less than the feed per tooth. The actual entry point trace is obtained by calculating force and workpiece deformation. Based on the shape characteristics of single-edge end milling tools analyzed by Yang [10] and the axial and radial contact tool-workpiece relationship proposed by Desai [11] as well as the elastic deformation theory of thin-walled parts, the expression of entry angle of micro-element is derived in the single-edge cutting process as follows:

$$\varphi_{\mathrm{en}}^{n} = \arcsin\left(\frac{R - a_e + \delta_m}{R}\right) \tag{7}$$

The entry angle $\varphi_{\mathrm{en}}^{n}$ of the j+1th element changes with the workpiece deformation δ_m. When $\varphi_{\mathrm{en}}^{n} - \varphi_{\mathrm{en}} \le d\varphi$, the micro-element cutting edge begins to participate in the cutting process. When $\varphi_{\mathrm{en}}^{n} - \varphi_{\mathrm{en}} > d\varphi$, the deformation is too large and the micro-element cutting edge does not contact the workpiece. It is inferred that the micro-element cutting edge does not participate in the cutting process. Therefore, the calculated workpiece deformation δ_m and rotation increment $d\varphi$ are the criteria for judging whether jth micro-element cutting edge is involved in cutting, as shown in Fig. 2:

When the jth tool teeth is cutting, the workpiece produces deformation δ_m, which causes the j+1th tool teeth to fail to reach the position of the cutting workpiece. Therefore, the actual entry angle $\varphi_{\mathrm{en}}^{n}$ of the j+1th tool teeth is calculated based on the deformation of the position.

3.2 Model for predicting instantaneous chip thickness

In the existing chip models, the calculation of cutting forces is based on undeformed chip thickness. In the milling process, with the change of tool rotation angle φ, the thickness of micro-element generated at each instantaneous angle φ will change accordingly.

The model of chip thickness change consists of two parts. The first part is the model of chip thickness. The instantaneous thickness change from small to large, and its expression is as follows:

$$h_j^1(\varphi_{\mathrm{en}} + (n-j)d\varphi) = R - \frac{(R - a_e) + \delta_{mj}(\varphi_{\mathrm{en}} + (n-j)d\varphi)}{\tan(\varphi_{\mathrm{en}} + (n-j)d\varphi)} \sqrt{\tan^2(\varphi_{\mathrm{en}} + (n-j)d\varphi) + 1} \quad (1 \le j \le n) \tag{8}$$

P is the projection of the intersection point of the element tangent thickness and the unmachined surface in the feeding direction, A is the position of the maximum instantaneous tangent thickness, and whether P and A cooperate again is the judgment condition of the first part instantaneous tangent thickness. The judgment expression is as follows:

$$P = \frac{(R - a_e) + \delta_{mj}(\varphi_{\mathrm{en}} + (n-j)d\varphi)}{\tan(\varphi_{\mathrm{en}} + (n-j)d\varphi)} \quad (P \ge R \cdot \cos(\varphi_{\mathrm{en}}) - f) \tag{9}$$

In the second part, the expression of instantaneous shear thickness model from large to small is as follows:

$$\varphi = \varphi_{en} + (n-j)d\varphi\,(1 \le j \le n)$$
$$h_j^2(\varphi) = R - \sqrt{\left(R^2 + f^2 + \delta_{mj}^2\right) + 2\left(f\cos\varphi - \delta_{mj}\sin\varphi\right)^2 + 2\left(f\cos\varphi - \delta_{mj}\sin\varphi\right)\sqrt{R^2 - \left(f\sin\varphi + \delta_{mj}\cos\varphi\right)^2}} \tag{10}$$

Q is the projection of the intersection point of the tangential thickness of the element and the machined surface in the feeding direction. The judgment expression of Q from point A to the cutting of the workpiece is as follows:

$$Q = \cos\varphi\left[\left(\delta_{mj}\sin\varphi - f\right) + \sqrt{R^2 - \left(f\sin\varphi + \delta_{mj}\cos\varphi\right)^2}\right] \quad \left(Q < R\cdot\cos(\varphi_{en}) - f\right) \tag{11}$$

The boundary of the thickness of the chip produced by the disc element at any one instant is based on the positions of P and Q, enabling a determination to be made as to whether the current tooth is involved in cutting (see Fig. 3).

When the intersection point P exists between the chip thickness h and the unmachined surface, the chip thickness changes from small to large, and the chip thickness is calculated by Eq. (10). When the micro-element tool teeth rotate to point A, the instantaneous chip thickness is the largest. When the intersection point Q exists between the chip thickness h and the trace of the upper tool teeth, the chip thickness decreases from large to small, and the chip thickness is calculated by Eq. (12). When the chip thickness h does not intersect with the trace of the upper tool tooth, the micro tool tooth moves out of the workpiece.

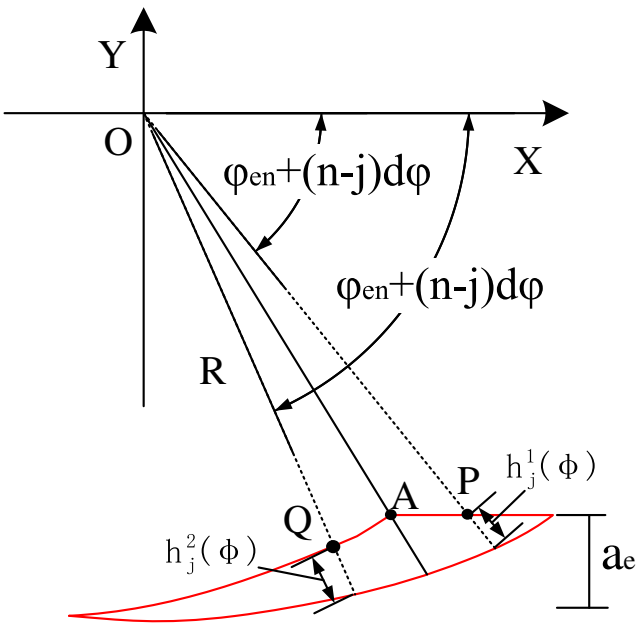

Fig. 3 Judging the thickness of the chip in relation to the disc element at any one instant

3.3 The relationship between milling force and workpiece deformation

When machining thin-walled parts, the workpiece is regarded as a weak rigid part and the cutting tool as a rigid part, so the deformation mainly occurs on the workpiece. In this paper, the relationship among instantaneous thickness h, instantaneous cutting force F, and workpiece deformation is analyzed, and then the coupling relationship between force and deformation of thin-walled parts is calculated, so that the surface error of thin-walled parts can be obtained. In the milling process of thin-walled parts, the deformation of workpiece is mainly caused by F_y. Therefore, the relationship between F_y and δ is studied in this paper. The solution process is as follows.

First of all, it is necessary to determine the functional relationship between the angular increment $d\varphi$ and the length of the axial disc element dz, as shown in the following equation:

$$d\varphi = \frac{\pi\cdot dz\cdot\tan\beta}{R} \tag{12}$$

The angle increment of each micro-element tool tooth involved in cutting is $d\varphi$. When the first $d\varphi$ is rotated by the tool tip, assuming that the workpiece does not deform, the instantaneous micro-element tangential thickness $[hj(\varphi_{en} + d\varphi), (j = 1)]$ and $F_{s,i,1}(\varphi_{en} + d\varphi)$ are calculated. The force at this time causes the deformation of the thin-walled parts to be $\delta_m,1(\varphi_{en} + d\varphi)$, which is calculated as the initial value, as shown in Figs. 4 and 5.

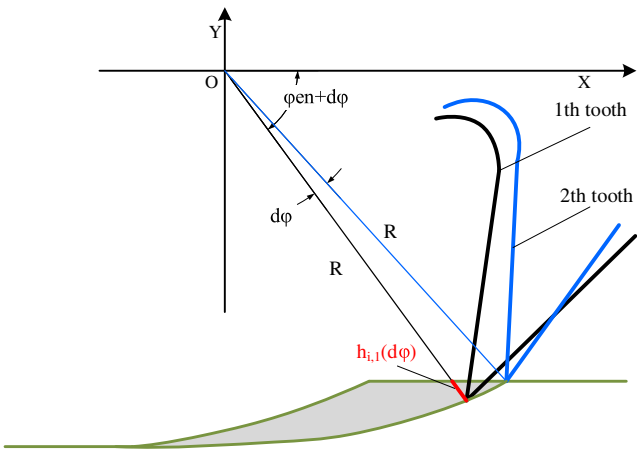

Fig. 4 First tooth chip thickness and the initial conditions

When the tool continues to rotate to a certain instantaneous position φ, the instantaneous cutting thickness h_j, cutting force F_y, and deformation of thin-walled parts can be obtained according to the initial value. By calculating the entry angle to determine whether micro-element cutting edge j participates in cutting, the instantaneous chip thickness boundary conditions P and Q are determined, and the matrix of delta δ_{mj} is obtained by iterative calculation method.

$$\delta_{mj}=\begin{bmatrix}
\delta_{m1}(\varphi_1) & 0 & 0 & \cdots & 0 & 0 & 0\\
\delta_{m1}(\varphi_2) & \delta_{m2}(\varphi_1) & 0 & \cdots & 0 & 0 & 0\\
\delta_{m1}(\varphi_3) & \delta_{m2}(\varphi_2) & \delta_{m3}(\varphi_1) & \cdots & 0 & 0 & 0\\
\vdots & \vdots & \vdots & \ddots & \vdots & \vdots & \vdots\\
\delta_{m1}(\varphi_{n-2}) & \delta_{m2}(\varphi_{n-3}) & \delta_{m3}(\varphi_{n-4}) & \cdots & \delta_{m(j-2)}(\varphi_1) & 0 & 0\\
\delta_{m1}(\varphi_{n-1}) & \delta_{m2}(\varphi_{n-2}) & \delta_{m3}(\varphi_{n-3}) & \cdots & \delta_{m(j-2)}(\varphi_2) & \delta_{m(j-1)}(\varphi_1) & 0\\
\delta_{m1}(\varphi_n) & \delta_{m2}(\varphi_{n-1}) & \delta_{m3}(\varphi_{n-2}) & \cdots & \delta_{m(j-2)}(\varphi_3) & \delta_{m(j-1)}(\varphi_2) & \delta_{mj}(\varphi_1)\\
0 & \delta_{m2}(\varphi_n) & \delta_{m3}(\varphi_{n-1}) & \cdots & \delta_{m(j-2)}(\varphi_4) & \delta_{m(j-1)}(\varphi_3) & \delta_{mj}(\varphi_2)\\
0 & 0 & \delta_{m3}(\varphi_n) & \cdots & \delta_{m(j-2)}(\varphi_5) & \delta_{m(j-1)}(\varphi_4) & \delta_{mj}(\varphi_3)\\
\vdots & \vdots & \vdots & \ddots & \vdots & \vdots & \vdots\\
0 & 0 & 0 & \cdots & \delta_{m(j-2)}(\varphi_n) & \delta_{m(j-1)}(\varphi_{n-1}) & \delta_{mj}(\varphi_{n-2})\\
0 & 0 & 0 & \cdots & 0 & \delta_{m(j-1)}(\varphi_n) & \delta_{mj}(\varphi_{n-1})\\
0 & 0 & 0 & \cdots & 0 & 0 & \delta_{mj}(\varphi_n)
\end{bmatrix} \tag{13}$$

4 Machining error prediction

Due to the deformation of thin-walled parts, the contact points on the workpiece surface deviate from those on the ideal contour. After considering the deformation of the workpiece and the points on the specified profile, the new position will be calculated according to the rotation angle position of the cutting edge. As a result, the simulated error surface caused by workpiece deformation error can be presented by the contact points obtained from each discrete position of the cutting edge transferring along the machining path, as shown in Fig. 6.

Considering the deflection of the thin plate, the contact point no longer stays on the straight line of the cutting edge but changes according to the change of the deflection of the thin-walled parts relative to the angle position of the cutting tool. Therefore, the milling surface is the trace of the contact point, which is a function of the tool angle position, and the coordinates on the *Y-Z* plane depend on the deformation of the workpiece (which is also a function). The trace of the contact point is shown in Fig. 6. In this case, the *Z* axis corresponds to the specified contour, and the trace of the contact point corresponds to the deformed contour. In this trace, two contact points 1 and 2 are considered. Their positions are determined by $\varepsilon_1(z_1, \varphi_1)$ and $\varepsilon_2(z_2, \varphi_2)$, which correspond to the angular positions of two cutting tools, φ_1, φ_2, and z_1 and z_2 along *Z* axis, respectively. The relationship between the angular position of the tool and the position *Z* is given by the following formula:

$$Z=\frac{R\varphi}{\tan\beta}\quad Z\in[0,\mathrm{ap}] \tag{14}$$

On the basis of the coupling relationship between workpiece deformation and milling force and the contact point relationship, the expression of ε_j is obtained.

$$\varepsilon_j=R-\left(\frac{R^2\tan\varphi}{\cos^2\varphi}-f^2\tan^3\varphi-\delta_{mj}\tan\varphi-2f\delta_{mj}\tan^2\varphi\right) \tag{15}$$

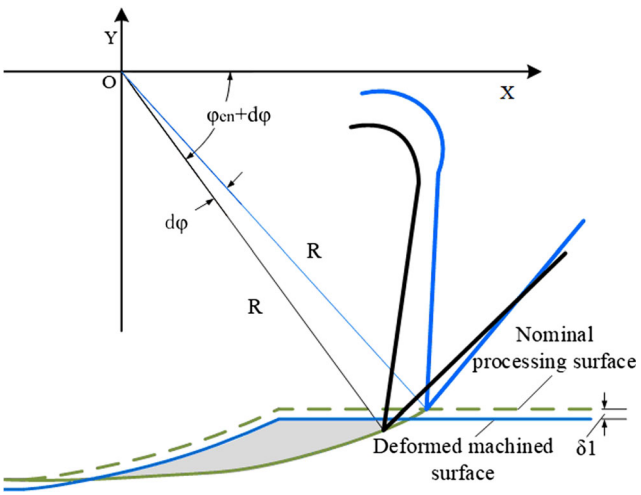

Fig. 5 The deformation of the workpiece according to the initial conditions

5 Experimental verification

5.1 Experimental setup

A measure experiment was carried out to verify the above analysis and compare the results to the predicted errors. The machine tool adopts VDL-1000E three-axis NC machine tool produced by Dalian Machine Tool. The cutter is flat-end

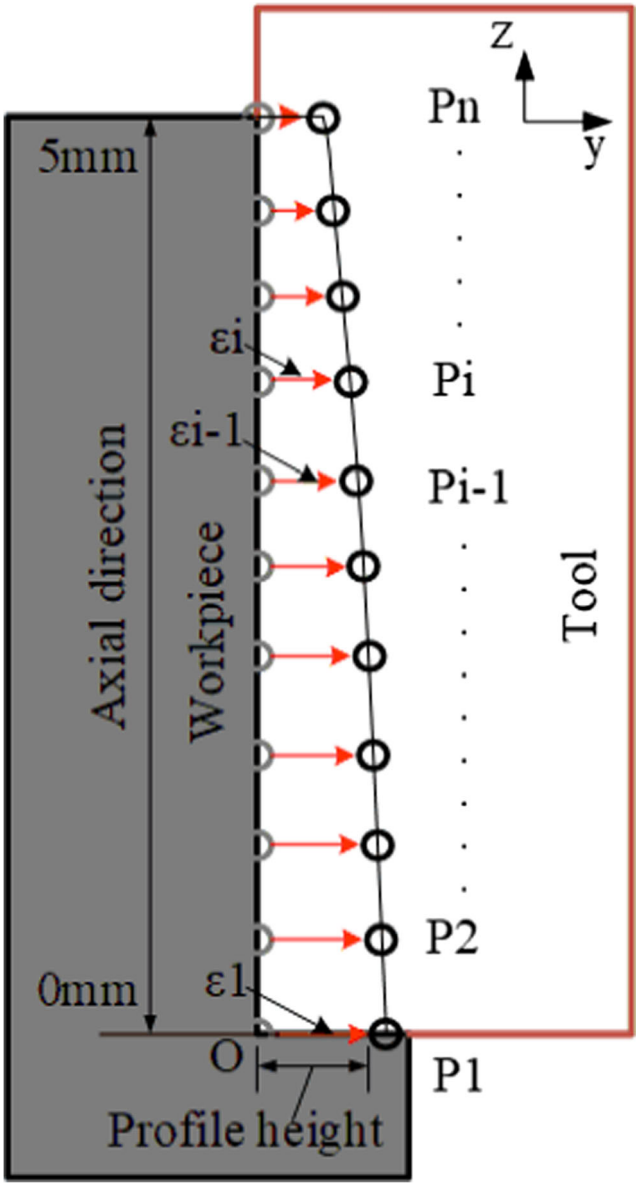

Fig. 6 Milled surface generated by the actual contact points resulting from deformation

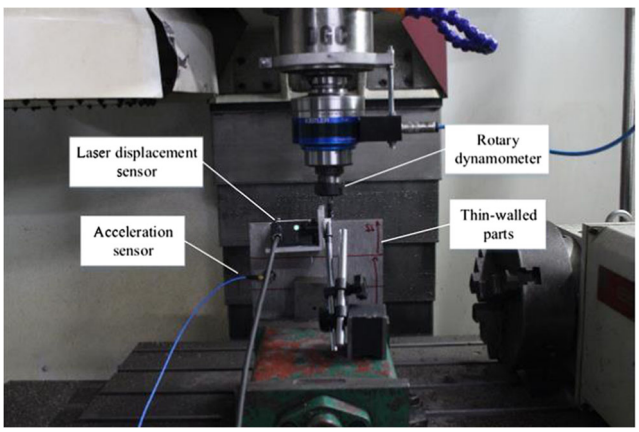

Fig. 7 Experimental setup

milling tool with 4 teeth and 10 mm diameter. The material of the workpiece is TC4 titanium alloy, and its size is 200 × 200 × 10 mm. Workpiece fixing length is 200 mm and extended length is 150 mm. Kistler 5236B rotary dynamometer and 5238B charge amplifier were used to collect cutting force signals during machining. Laser displacement sensor is used to measure the deformation of workpiece in the process of machining. A laser displacement sensor (KEYENCE LK-H020; sampling period 5 μs) was used to measure the amount of deformation of the workpiece. The selected single tooth feed was 0.04 mm, the machine tool spindle speed was 1000 r/min, the axial depth of cut was 5 mm, and the radial depth of cut was 0.4 mm. The experimental setup is shown in Fig. 7.

5.2 Prediction of milling force

Milling force is the most important parameter in the machining of thin-walled workpieces because it affects the quality and precision of the machined parts. The actual measured milling force of a certain period of time, the predicted milling force based on the variable chip thickness, and the milling force of the undistorted chip thickness are shown in Fig. 8.

From Fig. 8, it can be seen that the predicted peak value of the variable chip thickness of the feed direction milling force F_X is 8.3% lower than the average value of the measured peak value, while the calculated peak value of the undistorted chip milling force is 16.7% higher than the average value of the measured peak value. The predicted peak value of the radial milling force F_y was 6% lower than the average value of the measured peak value, and the calculated peak value of undeformed chip thickness is 15.3% higher than the average value of the measured peak value. It can be seen that in the actual milling process, the elastic deformation and the chip thickness decreases, so the force for undeformed chip thickness is larger thin-walled parts than the measured value. The error between the predicted milling force and the experimental value is small, which meets the requirements of the predicted results.

5.3 Prediction of surface shape

The machined surface profile produced during the experiment and the predicted surface profile are shown in Fig. 9. The machined surface was simulated using simulation parameters consistent with the test parameters. The machining error mainly changes along the axial direction of the tool. Coordinate measuring instrument was used for profile measurement. The predicted shape of the surface contour of the workpiece is in good agreement with the trend of the surface profile measured during experimental processing.

The contour shape obtained from the experimental data shows that the error deformation is large at the edge of thin-walled parts. The main reason is that the small stiffness at the edge of

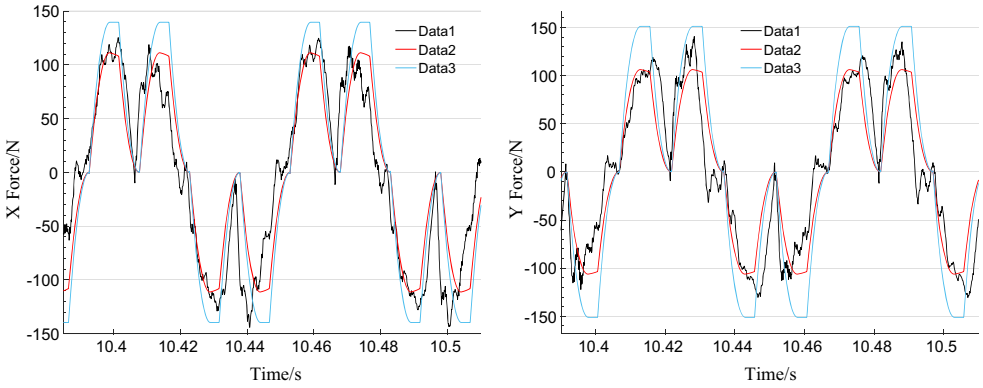

Fig. 8 Comparison of the experimental measurements and the predicted values for both variable chip thickness and undeformed chip thickness. Data 1—F_{exp}. Data 2—the predicted force with variable chip thickness. Data 3—the force for undeformed chip thickness. **a** X force. **b** Y force

workpiece will produce large deformation during the cutting process, and the average error value is 11%. When the tool moves along the feed direction, the workpiece strength increases and the deformation decreases, and the average error is less than 6%. The predicted contour is smooth without considering vibration, tool wear, and edge deformation of thin-walled parts. However, under the coupling effect of various factors in the actual processing process, the outline will appear obvious irregular shape.

A comparison between the experimental results regarding workpiece surface error and the theoretically predicted results are shown in Fig. 10.

The predictive values from P1 to Pn (Fig. 6) are compared with the measured values corresponding to the surface sizes of three different locations, as shown in Fig. 10. The surface error value of the cutting edge position of the micro-element which participates in cutting is larger than that of the micro-element cutting edge position which participates in cutting. This is because the number of micro-elements participating in the cutting process reaches the maximum, the resultant force of micro-elements cutting reaches the maximum, the deformation of thin-walled parts increases, and the surface error increases. When the micro-element cutting edge removes the workpiece one after another, the number of micro-elements involved in cutting decreases, the cutting resultant force decreases, the deformation of thin-walled parts decreases, and the surface error decreases accordingly.

Because of the complexity of edge cutting of thin-walled parts and the influence of other factors, there is a certain deviation between the model and the measured value. The average error of the predicted value of the tool tip position is less than 5%. The average error of the predicted value of the upper boundary position of workpiece is less than 10% because of the factors such as the smaller stiffness of workpiece and the vibration of workpiece. From the results, it can be seen that the trend of predicted and measured values coincides well, and the error difference at the edge of thin-walled parts is stable. The predicted workpiece deformation values are compared with the experimental data, as shown in Table 1.

6 Conclusions

This paper has presented a method for predicting milling force, elastic workpiece deformation, and surface errors based on the coupled relationship between milling force and deformation during the machining of thin-walled parts. According to the findings of this study, the following conclusions are drawn:

1. The deformation of the workpiece causes a change in the cutting contact relationship, resulting in a change in both the cutting trace of the disc element and the geometry of uncut chips. Based on the relationship between workpiece

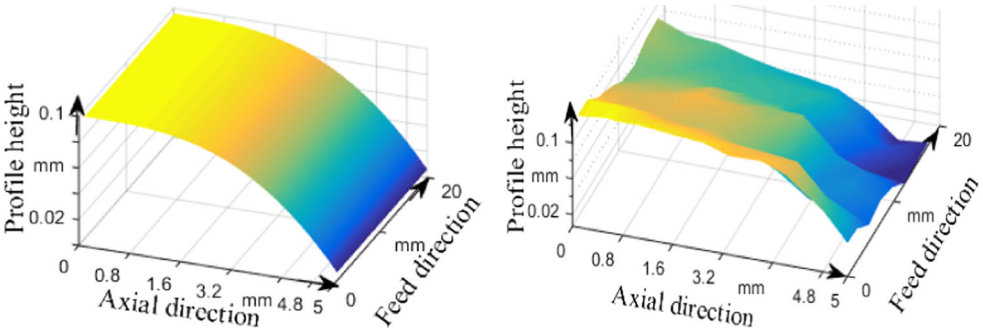

Fig. 9 Predicted surface profile and experimentally machined surface profile. **a** Theoretical prediction of the surface contour. **b** Experimentally produced surface contour

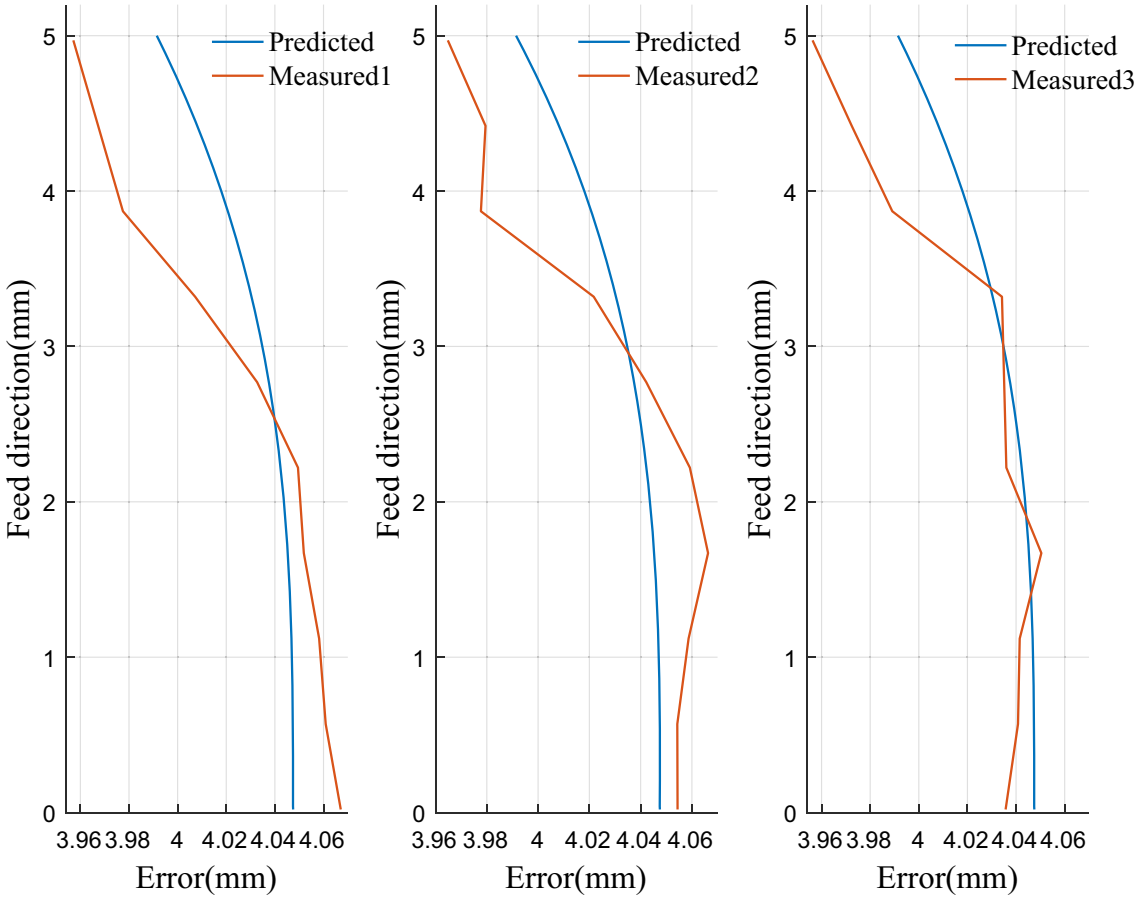

Fig. 10 Comparison of measured error and predicted error

deformation and micro-element contact, the expression of entry angle φ_{en} and the path of entry point are deduced, and the entry angle is predicted as the condition for judging whether micro-element cutting edge is involved in cutting. Cut-out angle φ_{ex} is obtained by iteration calculation of instantaneous chip thickness and workpiece deformation.

2. The variable chip thickness model of thin-walled parts is established by the elastic deformation δ, and the geometric boundary conditions of variable chip thickness are set up. Based on the instantaneous rigid force model, the relationship among instantaneous thickness h, instantaneous cutting force F, and workpiece deformation δ is obtained. Given the initial calculation conditions, the cutting force F_x, cutting force F_y, and matrix of workpiece deformation δ_{mj} under variable chip thickness is obtained.
3. The surface error changes of feed direction and axis are calculated by using workpiece deformation matrix and surface generation mechanism. Experiments verify the surface error results of the theoretical model. The

Table 1 Workpiece deformed results

No.	Time (s)	Simulation deformation (μm)	Measured values (μm)	Error (%)
1	10.4813	0.6	0.69	13
2	10.4826	2.2	2.5	12
3	10.4839	6.6	5.9	−6
4	10.4852	9.1	10.1	9
5	10.4865	7.8	8.6	9
6	10.4878	5.7	6.6	13.6
7	10.4891	3.4	3.9	12.8
8	10.4904	2	2.3	13
9	10.4917	0.9	1.1	18
10	10.4930	0.3	0.36	16.7

mismatch between the predicted error and the experimental results in the feed direction of the workpiece was 11%, but less than 6% for the start and middle positions. The mismatch for the predicted error value in the axial direction was less than 5% at the depth of cut position and less than 10% at the upper boundary of the workpiece. The trend of the prediction curve has a high degree of coincidence with the actual measured values.

When calculating instantaneous chip thickness, the trace of the upper tooth is an idealized circular path, so there is a certain deviation from reality in the chip thickness model. In this paper, we focused on single flute cutting relationships, so multi-flute cutting relationships were not analyzed. Therefore, it is necessary to further discuss the complex cutting relationship.

Funding information This project is supported by Projects of International Cooperation and Exchanges NSFC (51720105009).

References

1. Wan M, Zhang WH, Qin G, Tan G (2007) Efficient calibration of instantaneous cutting force coefficients and runout parameters for general end mills. Int J Mach Tools Manuf 47(11):1767–1776
2. Wan M, Zhang WH (2006) Efficient algorithms for calculations of static form errors in peripheral milling. J Mater Process Technol 171(1):156–165
3. Ratchev S, Liu S, Huang W, Becker A (2004) Milling error prediction and compensation in machining of low-rigidity parts. Int J Mach Tools Manuf 44(15):1629–1641
4. Chen D, Zhang XJ, Xie YK, Zhang XM, Ding H (2017) A unified analytical cutting force model for variable helix end mills. Int J Adv Manuf Technol 92(9–12):1–19
5. Gao YY, Ma JW, Jia ZY, Wang FJ, Si LK, Song DN (2016) Tool path planning and machining deformation compensation in high-speed milling for difficult-to-machine material thin-walled parts with curved surface. Int J Adv Manuf Technol 84(9–12):1757–1767
6. Li ZL, Tuysuz O, Zhu LM, Altintas Y (2018) Surface form error prediction in five-axis flank milling of thin-walled parts. Int J Mach Tools Manuf 128:21–32
7. Lin Z, Yang C, Peng F, Rong Y, Deng B, Ming L (2018) Prediction of flexible cutting forces and tool deflections for general micro end mill considering tool run-out and deflection feedback. Int J Adv Manuf Technol 96(1–4):1415–1428
8. Budak E, Tunç LT, Alan S, Özgüven HN (2012) Prediction of workpiece dynamics and its effects on chatter stability in milling. CIRP Ann Manuf Technol 61(1):339–342
9. Budak E, Altintas Y (1995) Modeling and avoidance of static form errors in peripheral milling of plates. Int J Mach Tools Manuf 35(3):459–476
10. Yang L, DeVor RE, Kapoor SG (2005) Analysis of force shape characteristics and detection of depth-of-cut variations in end milling. J Manuf Sci Eng 127(3):454–462
11. Desai KA, Rao PVM (2012) On cutter deflection surface errors in peripheral milling. J Mater Process Technol 212(11):2443–2454
12. Denkena B, Krüger M, Bachrathy D, Stepan G (2012) Model based reconstruction of milled surface topography from measured cutting forces. Int J Mach Tools Manuf 54:25–33
13. Zheng L, Liang SY, Zhang B (1998) Modelling of end milling surface error with considering tool-machine-workpiece compliance. J Tsinghua Univ 38:76–79
14. Zhang Z, Zheng L, Li Z, Zhang B (2001) Analytical model for end milling surface geometrical error with considering cutting force/torque. Chin J Mech Eng 37(1):6–10
15. Kline WA, DeVor RE, Shareef IA (1982) The prediction of surface accuracy in end milling. J Eng Ind 104(3):272–278
16. Song G, Li JF, Sun J (2013) Analysis on prediction of surface error based on precision milling cutting force model. J Mech Eng 49(21):168–170
17. Eksioglu C, Kilic ZM, Altintas Y (2012) Discrete-time prediction of chatter stability, cutting forces, and surface location errors in flexible milling systems. J Manuf Sci Eng 134(6):061006
18. Yue CX, Gao HN, Liu XL, Liang SY, Wang LH (2019) A review of chatter vibration research in milling. Chin J Aeronaut. https://doi.org/10.1016/j.cja.2018.11.007
19. Dépincé P, Hascoet JY (2006) Active integration of tool deflection effects in end milling. Part 1. Prediction of milled surfaces. Int J Mach Tools Manuf 46(9):937–944
20. Wan M, Zhang WH (2006) Calculations of chip thickness and cutting forces in flexible end milling. Int J Adv Manuf Technol 29(7–8):637–647
21. Altintaş Y, Lee P (1996) A general mechanics and dynamics model for helical end mills. CIRP Ann 45(1):59–64
22. Qi HJ, Zhang DW, Cai YJ, Shen Y (2010) Modeling methodology of flexible milling force for low-rigidity processing system during high speed milling. J Tianjin Univ 43(2):143–148